Earth and Planetary Science Letters 295 (2010) 231–240

Contents lists available at ScienceDirect

Earth and Planetary Science Letters

journal homepage: www.elsevier.com/locate/epsl

Dynamics and internal structure of the Hawaiian plume

Cinzia G. Farnetani [a,*], Albrecht W. Hofmann [b,c]

[a] Equipe de dynamique des fluides géologiques, Institut de Physique du Globe de Paris, and Université Paris Diderot, Paris, France
[b] Max-Planck-Institut für Chemie, 55020 Mainz, Germany
[c] Lamont-Doherty Earth Observatory, Columbia University, Palisades, NY 10964, USA

ARTICLE INFO

Article history:
Received 8 December 2009
Received in revised form 9 March 2010
Accepted 6 April 2010
Available online 1 May 2010

Editor: Y. Ricard

Keywords:
plume dynamics
Hawaii
HSDP
mantle heterogeneities

ABSTRACT

A thorough understanding of the internal structure of the Hawaiian plume conduit requires to link geochemical observations of surface lavas to fluid dynamic simulations able to quantify the flow trajectories of upwelling geochemical heterogeneities and their sampling by volcanoes. With the present work we fill a gap between the numerous geochemical studies of Hawaiian lavas and the paucity of dynamical models that relate the observed geochemical record to the internal plume structure. Our three-dimensional numerical simulation of a vigorous plume sheared by a fast moving oceanic plate shows that the dominant deformation in the conduit is vertical stretching, while horizontal spreading and vertical shortening prevail in the sublithospheric part of the plume (hereafter referred to as plume head). Flow trajectories indicate that a young volcano like Loihi samples the 'upstream' side of the plume, not its center, whereas volcanoes in the post-shield phase sample deep melts from the 'downstream' side of the plume. To constrain the internal conduit structure we focus on two geochemical observations: old (>350 kyr) Mauna Kea lavas from the Hawaii Scientific Drilling Project are isotopically distinct from recent Mauna Kea lavas, but they are isotopically identical to present-day Kilauea lavas. By modelling a plume conduit with several long-lasting filaments of 10 km radius, we find that the isotopic record of a volcano (e.g., Mauna Kea) is expected to change over time-scales of ~400 kyr. Furthermore, by requiring that two age progressive volcanoes (e.g., Mauna Kea and Kilauea) sample the same filament, we constrain the minimum filament length to be ~600 km. In this paper we adopt a 'top-down' approach: from geochemical observations of surface lavas, to dynamical models of the conduit structure, and further down to the 'geochemical architecture' of the thermal boundary layer feeding the plume. A conduit structure with filaments maps back into heterogeneous volumes with azimuthal and radial extents of several hundred kilometers in the source region of plumes.

1. Introduction

The age progressive Hawaiian–Emperor volcanic chain is arguably the best-documented example of a vigorous and long-lived intraplate volcanism caused by a mantle plume (Morgan, 1971). Due to the fast motion of the Pacific plate, the Hawaiian lavas provide us with a 'semi-continuous' chemical record of the underlying plume. Numerous geochemical and petrological studies (Hauri, 1996; DePaolo et al., 2001; Blichert-Toft et al., 2003; Eisele et al., 2003; Huang and Frey, 2003; Abouchami et al., 2005; Bryce et al., 2005; Sobolev et al., 2005; Garcia et al., 2006; Herzberg, 2006; Ren et al., 2006; Blichert-Toft and Albarède, 2009) investigated the complex spatio-temporal evolution of the erupted lavas, whereas the dynamics of a plume sheared by surface plate motion has been investigated numerically (Ribe and Christensen, 1994; Moore et al., 1998; Ribe and Christensen, 1999; Steinberger, 2000; van Hunen and Zhong, 2003) and with laboratory experiments (Richards and Griffiths, 1988; Kerr and Mériaux, 2004; Kerr and Lister, 2008). However, we still lack detailed dynamical models that relate the observed chemical record to the internal plume structure. To this end, we conduct three-dimensional numerical simulations of a vigorous thermal plume upwelling in the upper mantle and spreading beneath a fast moving oceanic lithosphere. The modelled internal conduit structure is based on Farnetani and Hofmann (2009), where we showed that deep seated passive heterogeneities rising in the plume conduit are stretched into 'filament-like' structures. Here we explore how such filaments may be sampled by a series of volcanoes. Before presenting the specific questions addressed in this paper we briefly review some key aspects of the Hawaiian volcanism.

Hawaiian volcanoes younger than 3 Ma form two parallel volcanic chains (Fig. 1), generally referred to as the Kea and Loa trends (Jackson et al., 1972). The trends are isotopically distinct and the overlap in lead isotopes is minor (Abouchami et al., 2005). Two components dominate: the relatively depleted Kea-component, probably derived from recycled, hydrothermally altered ultramafic lower oceanic crust and lithospheric mantle (Lassiter and Hauri,

* Corresponding author.
E-mail addresses: cinzia@ipgp.fr (C.G. Farnetani), albrecht.hofmann@mpic.de (A.W. Hofmann).

0012-821X/$ – see front matter © 2010 Elsevier B.V. All rights reserved.
doi:10.1016/j.epsl.2010.04.005

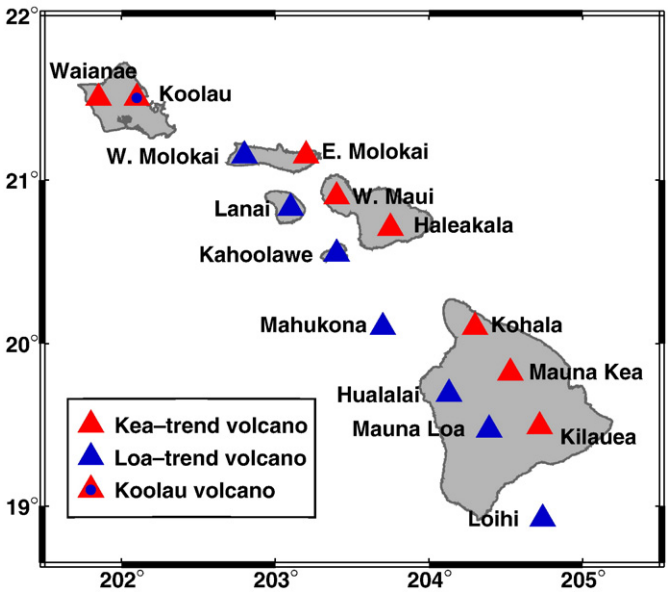

Fig. 1. Map of Hawaiian volcanoes.

1998), and the relatively enriched Koolau (extreme Loa)-component, composed of recycled oceanic crust and sediments (Lassiter and Hauri, 1998; Blichert-Toft et al., 1999). Melt inclusions in Mauna Loa olivines indicate the presence of ancient recycled oceanic crust (Sobolev et al., 2000), and the proportion of recycled crust was estimated by Sobolev et al. (2007) at about 20% of the Mauna Loa source. Interestingly, Loa-type lavas appeared only 3 Ma ago (Tanaka et al., 2008). Therefore, a time-invariable, concentrically zoned plume structure (Hauri et al., 1996; Lassiter et al., 1996), where Loa-type material upwells in the conduit center and Kea-type in the periphery, cannot explain either the sudden appearance of Loa-type lavas, or the distinctive isotopic fingerprints of Loa and Kea-trend volcanoes. Instead, over the last few million years the large-scale conduit structure probably showed a bilateral asymmetry (Abouchami et al., 2005).

Besides this large-scale geochemical difference, there is also a considerable variability between volcanoes belonging to the same trend. The Hawaii Scientific Drilling Project (HSDP) enabled otherwise inaccessible lavas to be studied, thus providing a unique record of time and space variability within Kea-trend volcanoes (Blichert-Toft et al., 2003; Eisele et al., 2003; Bryce et al., 2005; Blichert-Toft and Albarède, 2009). On the basis of lead isotope similarities between recent Kilauea and old (>350 kyr) Mauna Kea, Abouchami et al. (2005) propose an internal conduit structure with distinct and long-lasting compositional 'streaks'.

In contrast, (Blichert-Toft et al. (2003) suggested minor deformation and shearing across most of the conduit. This was due to the assumed 'plug-flow' velocity profile, which confines high velocity gradients to the conduit edge. Recently, Blichert-Toft and Albarède (2009) used a more appropriate vertical velocity profile, the one given by Olson et al. (1993), and found that weakly sheared heterogeneities are restricted to the conduit center. However, an important conclusion of Farnetani and Hofmann (2009) is that the study of deformation should not be limited to the conduit, where simple shear dominates, but it must include the converging flow at the base of the plume, where pure shear dominates. As shown by Manga (1996), pure shear is extremely efficient at stretching, explaining why axial heterogeneities are also considerably elongated (Farnetani and Hofmann, 2009).

Another important aspect is that Blichert-Toft and Albarède (2009) invoke cross-conduit mixing to explain the 'white-noise' portion of the isotopic fluctuation spectrum in the HSDP core. These relatively rapid geochemical fluctuations are not addressed in the present paper, which instead focuses on the 'low-frequency' systematic trends seen on lengths scales of tens of kilometers and time-scales of 100 kyr and greater (Abouchami et al., 2005). If cross-conduit mixing does indeed occur on small scales, it has clearly not significantly affected the larger scales considered in this paper.

Finally, the model by Bianco et al. (2008) proposes that small-scale heterogeneities are uniformly distributed within the conduit. Even in such a case, the Hawaiian volcanic chains can be geochemically distinct if: (a) heterogeneities have a lower solidus than the surrounding mantle. (b) Loa and Kea-trend volcanoes sample, respectively, the center and the extreme periphery of the conduit. In the framework of a concentric conduit, a Loa-trend volcano samples the plume center, but in its early and late phases the volcano must also sample the plume periphery, ideally acquiring a Kea-trend fingerprint. However, this model is not supported by recent isotope data (Hanano et al., 2010) on post-shield lavas from the Loa-trend volcanoes Hualalai and Mahukona, which conform to the distinctive Loa-trend isotopic compositions rather than resembling Kea-trend lavas. The work by Hanano et al. (2010) strongly reinforces the conclusions of Abouchami et al. (2005) that the plume is isotopically asymmetrical on a 50 to 100 km scale, rather than being 'uniformly isotopically heterogeneous' as assumed by Bianco et al. (2008).

The variety of geochemical models presented above contrasts with the paucity of dynamical models of the Hawaiian plume, which have generally focused on plume–lithosphere interaction (Moore et al., 1998) or estimated physical plume parameters using constraints from the observed topographic swell and geoid anomaly (Ribe and Christensen, 1994; van Hunen and Zhong, 2003). Ribe and Christensen (1999) provide melting rates and the volcano growth for a plume with a relatively low buoyancy flux ($B \sim 3000$ kg s^{-1}) compared to estimates for Hawaii, whereas they did not investigate the geochemical and isotopic evolution of surface lavas. According to the fluid dynamics laboratory experiments by Kerr and Mériaux (2004) the Hawaiian plume conduit should be azimuthally zoned. However, experiments have not evaluated the effects of partial melting, nor how a surface volcano samples a heterogeneous plume.

In this paper we model a Hawaiian plume and use the three-dimensional velocity field to advect passive (i.e., not affecting the flow) heterogeneities. By 'heterogeneity' we mean a volume of mantle rock which, upon melting has, on average, a specific isotopic composition. We investigate how heterogeneities deform during upwelling in the conduit and how their shape varies as a function of the initial position (central and peripheral) in the plume stem. To predict how heterogeneities are sampled by moving volcanoes we calculate the zone of partial melting and the volcano magma capture zone, where, ideally, plume melts rise vertically to the overlying volcanic edifice. We then address two main questions: (1) What are the time-scales over which we can expect a clear modification of the lava's geochemical fingerprint, due to successive sampling of different filaments? (2) What is the minimum filament length allowing two successive volcanoes (as identified by Mauna Kea and Kilauea) to sample the same filament? Finally, we model the sudden off-center arrival of Loa-type material (Tanaka et al., 2008), to investigate how volcanoes change their geochemical fingerprint and we estimate the size of deep mantle heterogeneities involved.

2. Numerical model

We use the three-dimensional Cartesian code Stag3D by Tackley (1998) to solve the equations governing conservation of mass, momentum and energy for an incompressible viscous fluid at infinite Prandtl number. The size of our model domain is 2000:1000:1000 km in X:Y:Z directions and the uniform grid size is 7.8 km/cell. To simulate a moving plate we impose a surface velocity $V_x = 9$ cm/yr and open X-side boundaries. A thermal plume is generated at the bottom of the

model domain by a Gaussian potential temperature perturbation of radius $r=100$ km and $\Delta T=250$ °C. The potential temperature for the plume is $T_p=1570$ °C, in agreement with recent estimates for Hawaiian lavas (Putirka, 2005), whereas for the surrounding mantle $T_m=1320$ °C. Potential temperatures T are related to real temperatures $\overline{T}_{real}$ through the relation $\overline{T}_{real}=T\exp(g\alpha z/C_p)$, where the specific heat $C_p=1000$ J kg^{-1} K^{-1}, the thermal expansion coefficient $\alpha=4\times10^{-5}$ K^{-1}, $g=10$ m s^{-2} and z is depth.

Viscosity depends on potential temperature as:

$$\eta=\eta_m\exp\left[\frac{E}{R}\left(\frac{T_m-T}{T_mT}\right)\right], \quad (1)$$

where $\eta_m=3\times10^{21}$ Pa s is the mantle viscosity, the activation energy $E=430$ kJ mol^{-1} (Karato and Wu, 1993), and R the gas constant. This exponential law gives $\eta=6\times10^{18}$ Pa s for a plume excess temperature $\Delta T_p=250$ °C. Viscosity varies also with depth: the 80 km thick oceanic lithosphere has a maximum viscosity $\eta=3\times10^{22}$ Pa s and the underlying asthenosphere has $\eta=6\times10^{20}$ Pa s.

The calculated plume buoyancy flux is:

$$B_p=\int\rho\alpha(T-T_m)V_z\,dxdy, \quad (2)$$

where V_z is the upwelling velocity and $\rho=3300$ kg m^{-3} is the mantle density. We model a vigorous plume with $B_p=6400$ kg s^{-1}, a value in the range of Hawaiian buoyancy flux: $B_H=6200$ kg s^{-1} (Davies, 1988) and $B_H=8700$ kg s^{-1} (Sleep, 1990). The corresponding plume volume flux $Q_v=\int V_z dxdy=300$ m^3 s^{-1} and the heat flux carried by the plume is: $Q_h=(B_pC_p)/\alpha=1.6\times10^{11}$ W.

To calculate partial melting we use the dry solidus formulation by Katz et al. (2003): $\overline{T}_{solidus}=aP^2+bP+c$, where the pressure $P=\rho gz$ and a, b, c are constants. Given our plume potential temperature, partial melting starts at a pressure of ca. 5.5 GPa, whereas the frequently used solidus by McKenzie and Bickle (1988) predicts a shallower onset of melting (~4.5 GPa). We assume a constant melt productivity $dF/dP=0.8$ wt.%kbar^{-1}, in agreement with estimates by Iwamori et al. (1995) for melting in the 4–5 GPa pressure range. A million passive tracers are advected using Akima's (1996) interpolation method, in order to calculate the 3-D trajectories inside the melting zone and the cumulative melt produced along each trajectory. This provides us with a criterion to stop partial melting, since we assume that dF/dP becomes zero once the cumulative melt production of a tracer sums up to 10 wt.%. In other words, we consider that the peridotitic restite becomes too refractory to continue melting after it has produced 10 wt.% melt. This threshold is lower than the complete phase exhaustion criteria for batch melting of garnet peridotite, but it represents a plausible value if sodium is efficiently removed during fractional melting, thereby reducing the melt productivity of the residual rock (Sobolev et al., 2007). Moreover, melt fractions of 5–10 wt.% were estimated by Pietruszka and Garcia (1999) for historical Kilauea lavas.

2.1. Model limitations

Our simulation has two significant limitations: First, we do not model 'active' heterogeneities, although eclogitic rocks are expected to be denser and more viscous than the surrounding peridotite. Density and viscosity differences would certainly affect the flow and the deformation rates, but it is still unknown to which extent. According to Blichert-Toft and Albarède (2009) viscous nuggets in the conduit may perturb the laminar flow and induce a toroidal component that enhances stirring. This hypothesis has not yet been tested for fluids at low Reynolds number, such as the mantle. Moreover, recent experiments on the rheology of garnet (Kavner, 2007) and of eclogite (Jin et al., 2001) show that the viscosity contrast between eclogite and peridotite may be weaker than previously thought.

Second, our melting model is very simple. For example, we neglect the effect of different lithologies, such as eclogite, on the melting temperature and melt productivity, as well as reactions between deep eclogitic melts and solid peridotite, in spite of their importance to Hawaiian lavas (Sobolev et al., 2005). Moreover, we do not model melt extraction through porous flow, focused flow, stress-driven melt segregation (Holtzman et al., 2003), or channeling instabilities (Connolly and Podladchikov, 2007). While melt transport processes can affect trace element chemistry, especially the relative enrichment of incompatible elements (Spiegelman, 1996), it is not clear to what extent they also affect isotopic abundances, used here to define heterogeneous Hawaiian lavas. It is obvious that melt inclusions do provide evidence for complex, most likely small-scale melt extraction processes, the mechanical aspects of which are poorly understood at present. It is possible, and in our opinion likely, that the apparently random, small-scale isotopic fluctuations discussed by Blichert-Toft and Albarède (2009) are caused by time-variable, small-scale melt extraction channels. For the much larger-scale isotopic heterogeneities addressed in this paper, it seems reasonable to assume that their averages are sufficiently well reflected by the bulk melt compositions. This assumption is reinforced by the systematic nature and reproducibility of these larger-scale isotopic features as extensively documented in the literature. This, in our opinion, justifies neglecting the details of melting and melt extraction for the purpose of this paper.

3. Results

Our plume upwells in a 'mantle wind' driven by the surface plate motion, so that the entire upper mantle moves in the same direction as the plate. Although this may seem simplistic, it is reasonable to assume that beneath the Pacific plate the return flow occurs in the lower mantle. For example, global flow models by Steinberger and O'Connell (2003) show that the Pacific mantle in the northern hemisphere flows in the same direction of the surface plate at least down to 600 km depth. In our simulation, the 'upper mantle wind' deflects the long-lived plume conduit and tilts it 15–18° with respect to the vertical direction (Fig. 2a). A tilted conduit for the Hawaiian plume is in agreement with recent work by Steinberger et al. (2004), although our tilt is lower than the 37–51° predicted for Hawaii (Steinberger, 2000). The shear flow generated by the plate motion also advects the plume head downstream, similar to the laboratory experiments by Kerr and Mériaux (2004), producing a strongly asymmetric temperature distribution. The lateral half width of the plume head is $W_{1/2}\sim400$ km, a value in agreement with the lateral extent $W_{1/2}\sim500$–600 km of sublithospheric low velocity anomalies (Laske et al., 2007; Wolfe et al., 2009) and with the Hawaiian topographic swell $W_{1/2}\sim500$ km (Detrick and Crough, 1978).

3.1. Partial melting and volcano growth

The calculated melting zone (Fig. 3a) is ~200 km long, 25–50 km thick and the melting rate $\Gamma=V_z\rho^2g(dF/dP)$ is highest at its base, where the upwelling rate V_z is ~30 cm/yr, as discussed later. Fig. 3a shows three flow trajectories: the upstream one indicates that a young volcano, such as Loihi, does not sample the plume center but its upstream side. Material upwelling along the central trajectory starts melting ~60 km downstream and it is sampled by a more mature (shield phase) volcano, such as Kilauea. Finally, the downstream trajectory only grazes the bottom of the melting zone, since the horizontal flow dominates over upwelling. Clearly, the downstream side generates less melt than the upstream side, suggesting that the Pacific asthenosphere is 'polluted' by plume material that has undergone low-degree melting or no melting at all. The trajectories also indicate that post-shield volcanic activity is associated with deep,

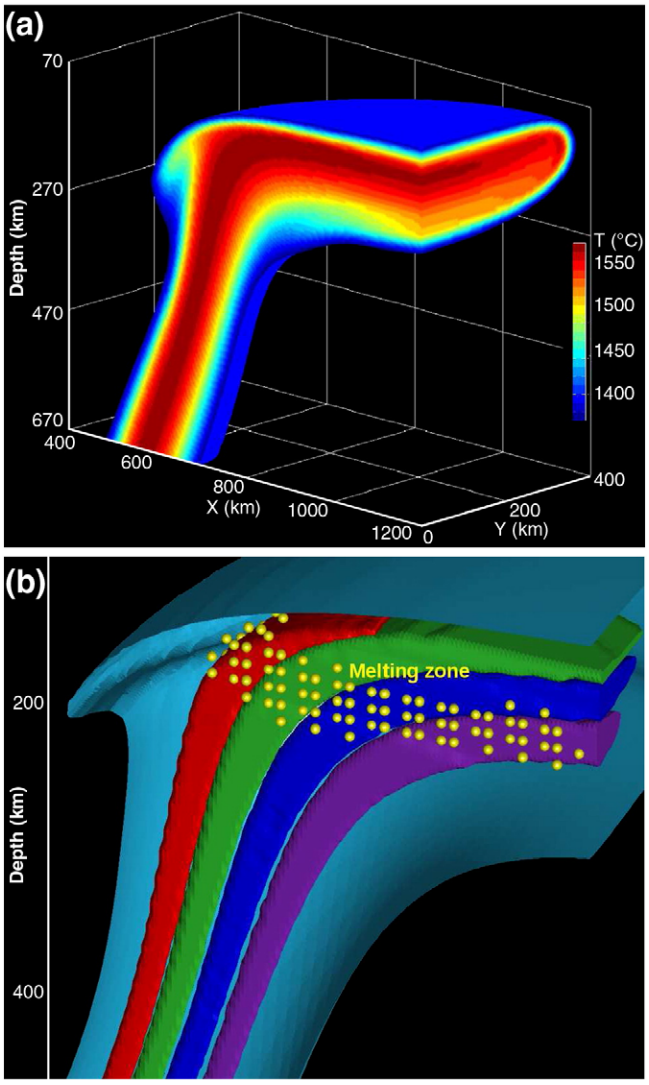

Fig. 2. (a) Three-dimensional view of the plume, only part of the computational box is shown. The plane at $Y=0$ is a plane of mirror symmetry. (b) Modelled internal structure with long filaments. Dots indicate the zone of partial melting.

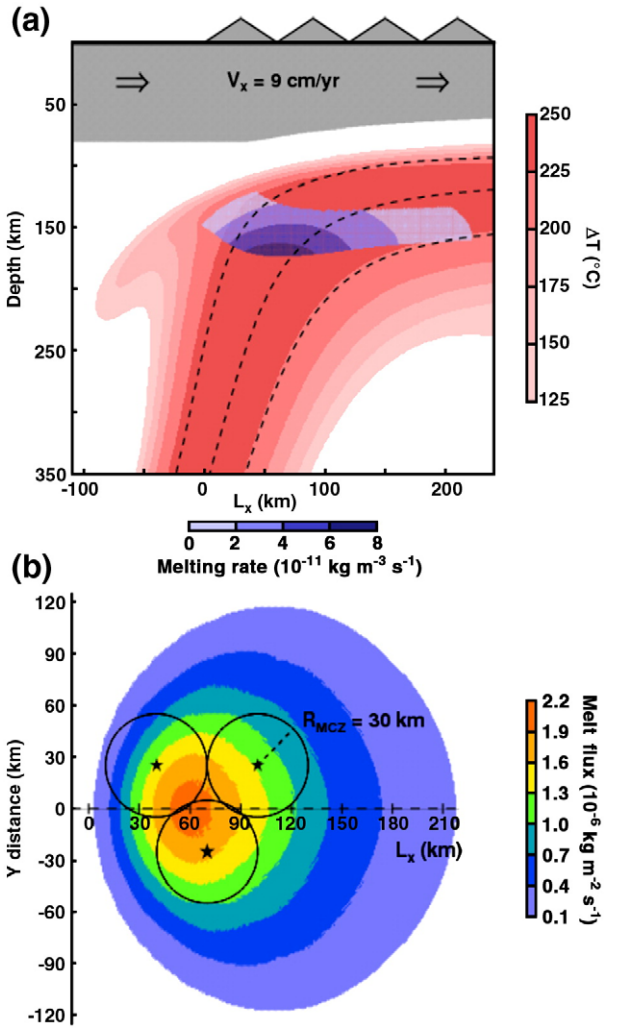

Fig. 3. (a) Vertical section at the plane of symmetry $Y=0$ km. Dashed lines indicate an upstream, a central and a downstream flow trajectory. Blue shades indicate the melting rate inside the melting zone. (b) Horizontal map of plume melt flux with circular magma capture zones of radius $R_{MCZ}=30$ km. Stars indicate the center of three off-axis volcanoes at a given time when the center coordinates (X_{MCZ}, Y_{MCZ}) are (40, 25), (100, 25) and (70, −25), respectively.

low-degree, alkaline melts formed downstream and coming from the underside of the plume. Although the nature of post-shield and of post-erosional volcanism is still a matter of debate, we note that Wirth and Rocholl (2003) found nanocrystalline diamonds in melt inclusions in garnet pyroxenite xenoliths on the Hawaiian island of Oahu. The genesis of diamonds requires a minimum pressure of 5 GPa and is consistent with the existence of low-degree melts formed at more than 150 km depth, as predicted by our model.

The map view of the melt flux $q=\int \Gamma dz$ (Fig. 3b) shows that q is greater than zero over an area of ~120 km radius, with highest values restricted to a central zone of ~40 km radius. The large lateral extent of the melting zone compares quite well with the 100–150 km half width of thickened Hawaiian crust (Watts and tenBrink, 1989). The plume melt production rate is: $M_p=\int(\Gamma/\rho_{melt})dV$, where the volume integral is over the entire melting zone and $\rho_{melt}=2700$ kg m^{-3}. Our value of $M_p=0.29$ km^3/yr is somewhat higher than the 0.2 km^3/yr estimated for Hawaii (Robinson and Eakins, 2006); however it is likely that only a fraction of M_p reaches crustal depths, thereby contributing to the volcano growth.

To evaluate the growth of a moving volcano we assume a circular magma capture zone (MCZ) of radius $R_{MCZ}=30$ km and center (X_{MCZ}, Y_{MCZ}), where X_{MCZ} varies with time, as the volcano is carried by the plate motion. We explore three possible values of Y_{MCZ}: 0, 25 and 50 km for a central, an off-center and an external volcano, respectively. Fig. 4a shows that the melt production rate inside the magma capture zone varies as a function of X_{MCZ} and the maximum values are 0.06 km^3/yr, 0.05 km^3/yr and 0.03 km^3/yr for a central, an off-center and an external volcano, respectively. Estimates for shield stage Kilauea vary from 0.05 km^3/yr (Quane et al., 2000) to 0.1 km^3/yr (Lipman et al., 2006), a difference in part due to the difficulty of dating potassium poor rocks. Our melt production rates are lower than that required to achieve a rapid (less than 1 Ma) volcano growth, which may be due to: (a) our assumption of dry peridotite partial melting, which neglects the contribution of more fertile components such as eclogite and/or hydrous peridotite, (b) our simplistic choice of a constant radius, circular magma capture zone, which, although generally assumed (DePaolo and Stolper, 1996; Ribe and Christensen, 1999) is not based on a thorough understanding of how deep partial melts converge to form a volcanic edifice. Our results indicate long durations (1.5 Ma) for a volcano growth, in better agreement with estimates around 1.2 Ma (Quane et al., 2000; Garcia et al., 2006), rather than 0.6 Ma (Moore and Clague, 1992).

The calculated cumulative melt volumes (Fig. 4b) for a central and an off-center volcano range between 75,000 and 65,000 km^3, such values are in general agreement with the volume of Mauna Loa

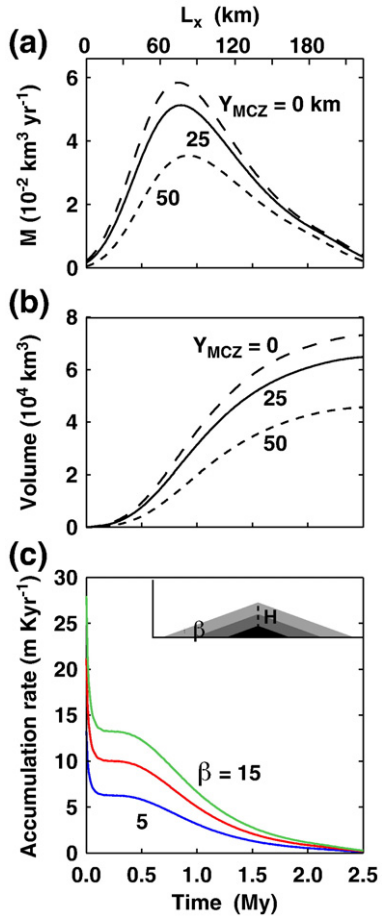

Fig. 4. (a) Melt production rate M vs. the length of the melting zone in the X direction (L_X) for a central volcano ($Y_{MCZ}=0$ km, long dashed line), an off-center one ($Y_{MCZ}=25$ km, solid line), and an external one ($Y_{MCZ}=50$ km, short dashed line). (b) Cumulative melt volume captured by the three volcanoes (lines as above). (c) Accumulation rates for a simple conical volcano (shown in the inset), for a volcano slope $\beta=15°$ (green), $\beta=10°$ (red), $\beta=5°$ (blue).

(74,000 km^3) and Haleakala (69,800 km^3) estimated by Robinson and Eakins (2006). Given the modest volume difference between volcanoes belonging to the Loa and Kea-trends, we consider that the schematic configuration with a double volcanic chain of off-center volcanoes (Fig. 3b) is more plausible than the configuration with a central and an external volcanic chain used by Bianco et al. (2008).

The three-dimensional shape of a Hawaiian volcano is quite complex, since the new edifice grows on the flanks of older ones (Lipman et al., 2006). Here we assume a simple conical shape and calculate the lava accumulation rates (Fig. 4c) for an off-center volcano. We consider a range of possible volcano slopes: $15°<\beta<10°$ is appropriate for early submarine growth, for example Loihi flanks unaffected by mass wasting dip ~14° (Garcia et al., 2006), whereas for subaerial growth $\beta<5°$. Calculated accumulation rates are around 10–15 m/kyr for underwater shield volcanism and 5 m/kyr for subaerial volcanism. Such values are lower than the 20–30 m/kyr estimated by DePaolo and Stolper (1996) but seem to agree better with the relatively low accumulation rates (~8 m/kyr) for the submarine part of the HSDP (Sharp and Renne, 2005) and with the ~10 m/kyr estimated by Lipman et al. (2006) for Kilauea tholeiitic lavas.

3.2. Vertical velocity field and deformations

In order to understand how heterogeneities are deformed during upwelling in the conduit we consider the velocity field and the associated strain rates. Fig. 5a shows the vertical velocity V_z inside the plume. V_z varies radially across the conduit and the high velocity gradient dV_z/dr induces a strain rate $\dot{\varepsilon}_{rz}$ with maximum values $\dot{\varepsilon}_{rz}^{max}=4\times10^{-13}$ s^{-1} at radial distances of 30–40 km (see inset). Moreover, V_z decreases upwards along a given flow trajectory, and this has two important implications. First, V_z inside the melting region is 25–50% lower than in the deep conduit. Therefore, upwelling velocities estimated from uranium series disequilibria in the shallow part of the plume (e.g., Bourdon et al., 2006) should be extrapolated with care to the deep conduit. Second, the observed V_z reduction is accompanied by horizontal spreading of the upwelling material. The velocity gradients (e.g., dV_z/dz, dV_y/dy) associated with the vertical slowdown and horizontal spreading of the plume head induce strain rates that deform the heterogeneities. A simple way to visualize the effect of strain rates is to advect half-spheres, whose vertical section on the plane $Y=0$ is a circle of 10 km diameter, initially placed at 500 km depth (Fig. 5b). The central half-sphere upwells quite undeformed (low $\dot{\varepsilon}_{rz}$), but eventually undergoes vertical shortening (high $\dot{\varepsilon}_{zz}$) and horizontal spreading. When it enters the melting zone it has a flattened shape, ~20 km wide and ~3.5 km thick. In contrast, the half-spheres at the upstream and downstream side are stretched into 'filaments' ~60 km long and only 1 km wide. The external half-sphere is the most elongated; this is not surprising since the elongation (i.e., the ratio of the length variation over the initial length) is directly proportional to the strain rate and to the time t during which $\dot{\varepsilon}_{rz}$ operates. At the conduit edge, $\dot{\varepsilon}_{rz}$ is low, but t is high (several Ma) due to the slow upwelling velocity. Given the different final shapes, the modelled volume elements also have different transit times inside the melting zone: ca. 0.4 Ma for the central one, and more than 1 Ma for the peripheral volume element.

3.3. Long filaments in the conduit

We have just shown that 'blob-like' (i.e., roughly equant) heterogeneities upwelling in the upper mantle conduit are readily stretched into filaments, except at the axis. A key question then is: How likely it is to find 'blob-like' heterogeneities inside a plume conduit? The answer is: quite unlikely. Farnetani and Hofmann (2009) show that heterogeneities embedded in the source region of plumes undergo considerable shear as they flow horizontally inside the thermal boundary layer (TBL) towards the base of the plume and as they rise in the conduit. Therefore, in the following we assume that heterogeneities upwelling from the lower- into the upper mantle have an elongated shape, and we model filaments with a circular cross section of radius $r=10$ km and length $L>1000$ km (Fig. 2b). We investigate how a single volcano carried by the oceanic plate samples the long-lived filaments crossing the melting zone (Fig. 6a) and we plot the melt production rate of each filament during the volcano lifetime (Fig. 6b). We note that at each time two or more filaments are simultaneously sampled, and that the geochemical fingerprint of the erupted lavas is expected to change clearly over distances of 40 km (e.g., at $X_{MCZ}=10$ km filament F1 dominates; at $X_{MCZ}=50$ km, F2; at $X_{MCZ}=90$ km, F3). The conclusion that a single volcano changes its geochemical fingerprint as it drifts over the plume is consistent with the findings that old Mauna Kea lavas have distinct and different Pb isotope ratios relative to recent lavas (Abouchami et al., 2005).

Abouchami et al. (2005) reveal another interesting observation: present-day Kilauea is isotopically identical to old Mauna Kea, and this led the authors to infer that the Hawaiian conduit should be composed of narrow and long-lived 'streaks'. Here we use this observation to constrain the minimum filament length so that two volcanoes belonging to the same chain can sample the same filament. We vary the filament initial length L_i at 660 km depth, and we find that if $L_i=300$ km (Fig. 7a), the older volcano (Mauna Kea, MK) dominantly samples the filament, whereas the younger one (Kilauea, K) will not, for two reasons: (i) in the uppermost mantle the filament undergoes

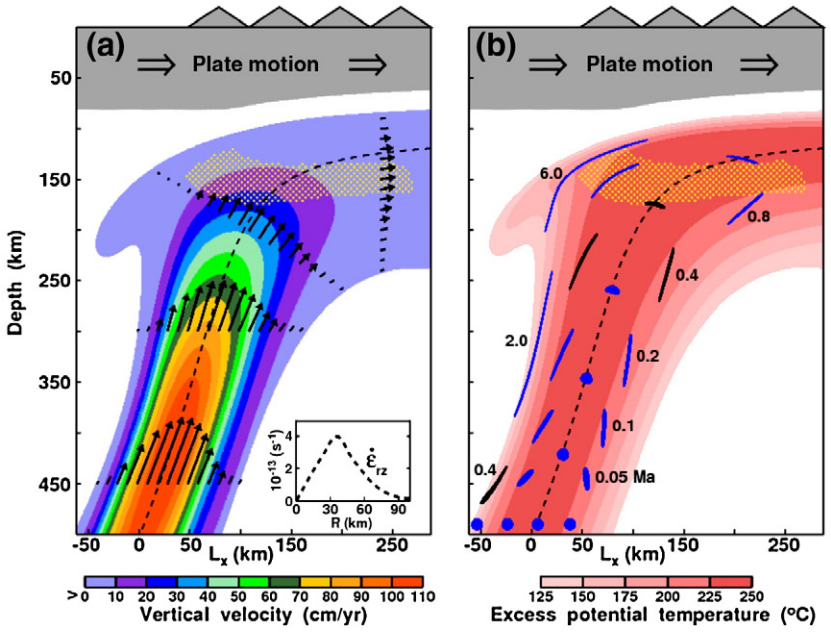

Fig. 5. (a) Vertical velocity component V_z is shown by color coding. For clarity, the x–z velocity field (arrows) is shown only at selected levels. Melting zone (dots) and a central flow trajectory (dashed line). Inset: radial distance across the plume conduit vs. strain rate. (b) Four passive heterogeneities with an initial shape of a half-sphere ($Y=0$ being the plane of mirror symmetry), and a diameter of 10 km, at the initial depth of 500 km. Their shape and position are plotted at different times. The rise times shown at the left (from 0.4 to 6 Ma) refer to the heterogeneity in the outer, leading margin of the plume. The rise times on the right (from 0.05 to 0.8 Ma) refer collectively to the downstream, the central and the upstream heterogeneities. The position of four heterogeneities after 0.4 Ma (black) enables to appreciate the different rise time inside the conduit.

shortening and horizontal spreading so that its vertical length dramatically decreases from ~150 km (Fig. 7d) to ~50 km (Fig. 7e, in light green). (ii) The filament is rapidly advected downstream because the horizontal velocity in the plume head is higher than the plate velocity ($V_x^{\text{plume}} \sim 3V_x^{\text{plate}}$). Therefore, the filament exits the zone of partial melting before being sampled by the younger (K) volcano. For the cases with $L_i=600$ km (Fig. 7b) and $L_i=900$ km (Fig. 7c) the younger volcano does sample the filament during its shield phase; moreover, the filament contribution to the melt production rate progressively increases with L_i. We conclude that a minimum filament length between 600 and 900 km is required to explain the geochemical observation presented above.

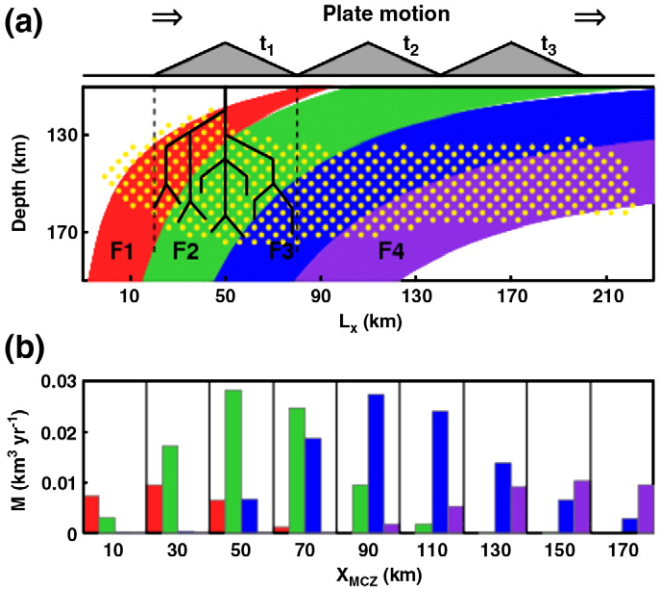

Fig. 6. (a) Filaments (F1 to F4) crossing the melting zone. The position of a single volcano is shown at different times (t_1–t_3). (b) Melt production rate of each filament calculated in the magma capture zone of the moving volcano, vs. volcano position X_{MCZ}.

3.4. Conduit bilateral asymmetry and its time evolution

The strong lateral isotopic contrast between Loa and Kea-trend volcanoes described by Abouchami et al. (2005) has been confirmed by Tanaka et al. (2008) and Hanano et al. (2010). However, according to Tanaka et al. (2008) the Loa-type geochemical fingerprint appeared only a few million years ago, during the Koolau shield stage. We therefore simulate a massive 'lateral' arrival of Loa-type filaments in the plume conduit and explore how volcanoes belonging to the same chain register the arrival (Fig. 8a), the transit (Fig. 8b), and the waning (Fig. 8c) of Loa-type material over time-scales of 2.5–3.0 Ma. The horizontal section of the plume conduit at 660 km depth (Fig. 8d) indicates the assumed lateral structure with several filaments of 5 km radius (upstream/downstream filaments in dark/light blue).

In Fig. 8e–g the Loa-type filaments are lumped together by a single blue signature and this blue area shows the total contribution of the bilateral Loa signature, whereas the solid and the dashed lines indicate the separate contributions of the upstream and downstream filaments, respectively. Fig. 8e shows that an old volcano (B, Waianae) is Kea-type, except in the late post-shield phase. For a younger volcano (C, Koolau), lavas in the shield stage are expected to change their geochemical fingerprint from purely Kea-type (red color) to a coexistence of Kea and Loa-type (Fig. 8f), whereas post-shield lavas should have a clear Loa-type geochemical fingerprint. Subsequent younger volcanoes, for example D (Lanai) and E (Kahoolawe) are expected to have Loa-type lavas both in the shield and post-shield stages (Fig. 8g). These predictions are in general agreement with the existence of Loa-type lavas in Kahoolawe (Huang et al., 2005) and Lanai (Tanaka et al., 2008), whereas for Waianae some undated Loa-type lavas have been found in the slump complex (Coombs et al., 2004).

According to Tanaka et al. (2008) the Loa geochemical signature is presently waning, as indicated by the tendency of Mauna Loa, and especially Loihi lavas toward less extreme isotope compositions. If this

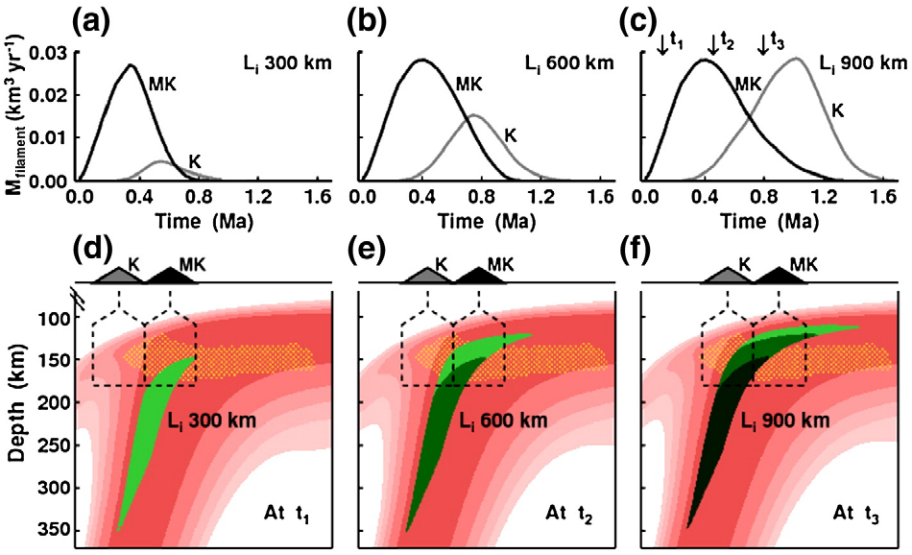

Fig. 7. Top: Time vs. filament melt production rate as registered by two volcanoes MK (Mauna Kea, black line) and K (Kilauea, gray line). (a) For filament initial length $L_i = 300$ km. (b) For $L_i = 600$ km. (c) For $L_i = 900$ km. A 300 km filament is only marginally sampled by Kilauea, whereas the 600 and 900 km filaments are well represented by Kilauea lavas. Bottom: 2D view of the plume, each shade of green keeps track of an initial filament length of 300 km. (d) Filament $L_i = 300$ km shown at time $t_1 = 0.1$ Ma ($t = 0$ marks the arrival of the filament in the melting zone). (e) Filament $L_i = 600$ km shown $t_2 = 0.45$ Ma. (f) Filament $L_i = 900$ km shown $t_3 = 0.8$ Ma.

indeed reflects the end of the Loa-type filaments (Fig. 8c), we conclude that these continuous filaments with a lifetime of 2.5 Ma must be at least 2000 km long in the plume conduit.

Our model certainly represents a gross simplification of the geochemical evolution within the Hawaiian plume, since we neglect that Loa-type material is probably enriched in fertile recycled crust. Moreover, we consider that Koolau geographically belongs to the Loa volcanic chain. However, the spatial separation between Loa and Kea-trends is not so obvious in this older part of the chain, and Koolau might have started as a volcano more closely centered on the plume track. In this case, a strictly bilateral conduit structure may fail to predict the extreme Loa fingerprint of the late Makapuu-stage lavas at Koolau (Fekiacova et al., 2007; Tanaka et al., 2008). Finally, there is evidence that Loa-like lavas may occur in Kea volcanoes, for example in Mauna Kea (Eisele et al., 2003) and Haleakala (Ren et al., 2006), and that melt inclusions occasionally have both Kea and Loa geochemical fingerprints (Ren et al., 2005). Our modelled bilateral conduit asymmetry does not preclude upwelling of Loa-type material also on the Kea side of the plume, albeit with shorter life times and reduced length-scales of heterogeneities.

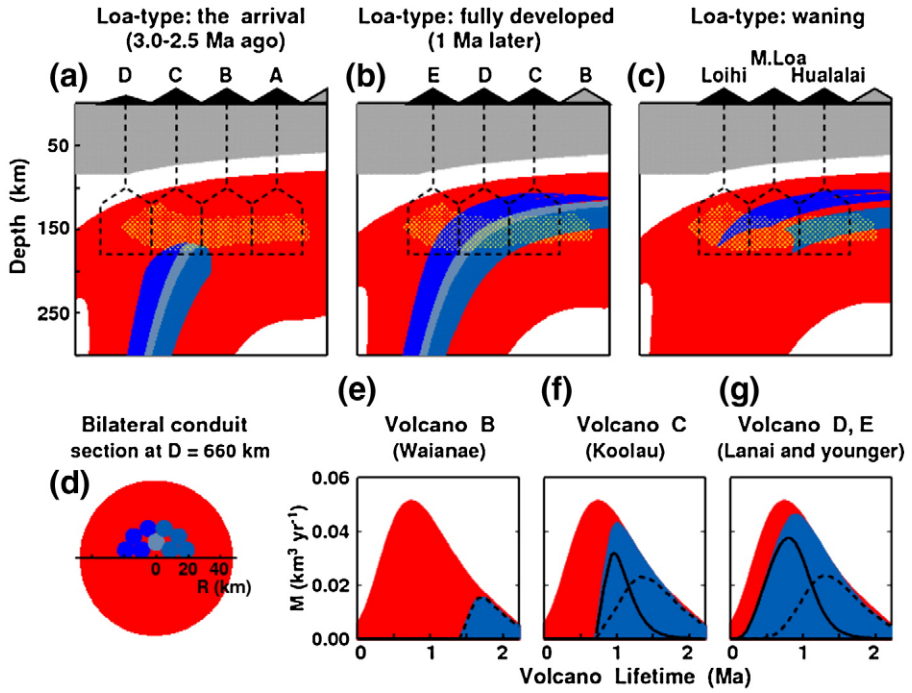

Fig. 8. Top: 2D view of the plume (red), with distinct Loa-type filaments (blue) shown at different stages. (a) Arrival. (b) Transit. (c) Waning. Bottom: (d) Horizontal cross section of the conduit with initial filament position. (e) Time vs. melt production rate for volcano B (Waianae). Contribution of all filaments (blue area), contribution of upstream filaments only (solid line), contribution of downstream filaments only (dashed line). (f) Same as above, for volcano C (Koolau). (g) Same as above, for younger volcanoes.

4. Tracing filaments backward in time

The results presented here and in our companion paper (Farnetani and Hofmann, 2009) enable us to adopt a new 'top-down' approach: from the geochemical variability of the surface lavas, to the plume conduit structure and further down to the 'geochemical stratigraphy' across the thermal boundary layer (TBL), the source region of plumes. We can thus attempt to elucidate the relation between length-scale of heterogeneities in the melting zone — as inferred from geochemical observations of the Hawaiian lavas — and the corresponding length-scale of heterogeneities in the lowermost mantle. We have found that the minimum length allowing two age progressive volcanoes to sample the same filament should be several hundred kilometers, and we now ask the following question: if an upper mantle filament is traced back into the lower mantle, what would be its size and shape once in the TBL?

In order to advect the filament backward in time we use the velocity field calculated by Farnetani and Hofmann (2009) for a vigorous lower mantle plume.[1] We investigate the effect of variations in filament length L_f (e.g., 500 and 1000 km), radius r_f (e.g., 5 and 10 km) and radial distance from the conduit center D_f (e.g., 0, 15 and 30 km). The inset of Fig. 9 shows the conduit cross section with the initial position of five filaments, whereas Fig. 9 shows the shape of each filament once traced back into the TBL. Filament A ($r_f = 10$ km, $L_f = 500$ km, $D_f = 30$ km) maps back into a fan shaped heterogeneity with a radial size of more than 300 km and a vertical thickness of less than 10 km. Filament B ($r_f = 5$ km, L_f and D_f as above) maps into a heterogeneous volume with lower radial (200 km) and azimuthal dimensions relative to the previous case. Filament C, identical to the above except for $D_f = 15$ km, maps into a heterogeneous volume with a considerable azimuthal extent and a radial size of order 100 km. This is not surprising, because filaments closer to the conduit center map back to a greater azimuthal extent and at a greater depth inside the TBL, as clearly shown by the central filament E, which maps into a deep annulus.

In conclusion, the conduit structure model with long-lived filaments implies the existence of large-scale heterogeneous zones in the TBL, with a radial size of several hundred kilometers and variable azimuthal extent. Our modelling is consistent with experiments by Kerr and Mériaux (2004), suggesting an azimuthal distribution of geochemical heterogeneities. In contrast to the above, some models of the Hawaiian conduit structure rule out the existence of large-scale heterogeneities in the TBL. For example, the concentrically zoned model with a plume center geochemically distinct from its periphery maps back into an horizontally stratified TBL (Farnetani and Hofmann, 2009), assuming negligible entrainment of surrounding mantle, as argued by Farnetani et al. (2002). Similarly, the 'uniformly heterogeneous' model by Bianco et al. (2008) implies a remarkably uniform vertical and azimuthal distribution of small-scale heterogeneities in the TBL.

5. Conclusion

Our numerical simulation has shown that:

1) A vigorous Hawaiian plume spreading beneath a fast moving oceanic lithosphere is expected to have a 15–18° tilted conduit of ~100 km radius and a maximum excess temperature of 250 °C. The plume head is strongly elongated in the direction of the plate motion and reaches a lateral half width of ~400 km. The plume head temperature anomaly extends from sublithospheric depths to more than 250 km depth, even far downstream from the plume conduit. Many of the modelled plume features agree with the extent of low seismic velocity anomalies recently detected by Wolfe et al. (2009) beneath the Hawaiian hotspot.
2) A young volcano like Loihi does not sample the plume center, but its front edge or 'upstream' side. Conversely, post-shield volcanism is associated with deep (5 GPa) melts formed 'downstream' and from the underside of the plume. By comparing the flux of plume material that undergoes partial melting $Q_{pm} = M_p \rho / \rho_{melt} = 0.35$ km^3/yr, to the total plume volume flux $Q_v = 9.4$ km^3/yr we conclude that only a small fraction (~4%) of the plume meets the pressure–temperature conditions to melt. Therefore, an important volume of pristine Hawaiian plume material is expected to 'feed' and to geochemically 'pollute' the Pacific asthenosphere (Phipps Morgan et al., 1995).
3) The calculated lava accumulation rates are 10–15 m/kyr for underwater shield volcanism and 5 m/kyr for subaerial volcanism. These values are lower than the 20–30 m/kyr estimated by DePaolo and Stolper (1996), but are in agreement with relatively low accumulation rates (~8 m/kyr) for the submarine part of the HSDP (Sharp and Renne, 2005) and with the ~10 m/kyr for Kilauea tholeiitic lavas (Lipman et al., 2006).
4) In the conduit, radial gradients of the vertical velocity (dV_z/dr) shear passive heterogeneities into elongated filaments, except at the plume axis where dV_z/dr is zero. In the plume head the vertical velocity decreases (by 25–50%) while the horizontal velocities increase. The associated strain rates induce a vertical shortening and horizontal spreading of the upwelling heterogeneities. We conclude that nowhere in the melting zone is it possible to find undeformed heterogeneities.
5) Using the results of Farnetani and Hofmann (2009) as a starting point, we model several long ($L \sim 1000$ km) and narrow ($r \sim 10$ km) filaments and calculate their trajectories and their contribution to the melt production. Given this input, a surface volcano will change its geochemical fingerprint, due to successive sampling of distinct filaments, over a distance of ~40 km (which corresponds to a time-scale of ~450 kyr for a plate velocity of 9 cm/yr). This agrees with the finding of Abouchami et al. (2005)) that present-day Mauna Kea is geochemically distinct from old (>350 kyr) lavas from the HSDP. We can thus explain the isotope trends over relatively long time-scales, but our model does not address the short time-scale fluctuations (e.g., 10 kyr) in the stratigraphic record of the HSDP, observed by Eisele et al. (2003) and elaborated by Blichert-Toft and Albarède (2009).

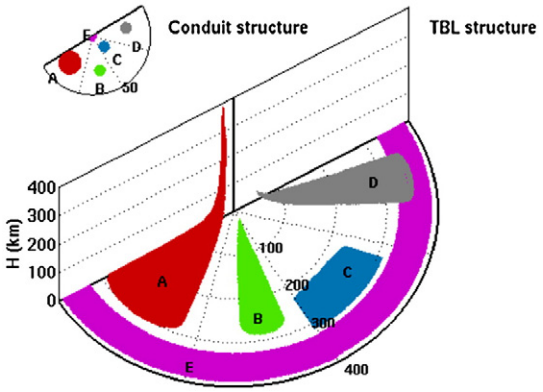

Fig. 9. Inset: conduit cross section with initial position of five filaments of radius r_f and length L_f, at radial distance D_f. (Filament A: $r_f = 10$ km, $D_f = 30$ km, $L_f = 500$ km. Filament B: $r_f = 5$ km, $D_f = 30$ km, $L_f = 500$ km. Filament C: $r_f = 5$ km, $D_f = 15$ km, $L_f = 500$ km. Filament D: $r_f = 5$ km, $D_f = 30$ km, $L_f = 1000$ km. Half-Filament E: $r_f = 5$ km, $D_f = 0$ km, $L_f = 500$ km). Main figure: backward tracing of the filaments in the thermal boundary layer (TBL) and the resulting radial and azimuthal structure of the TBL.

[1] The velocity field (V_r and V_z) in cylindrical axisymmetric geometry by Farnetani and Hofmann (2009) is easily recalculated onto a three-dimensional Cartesian grid (V_x, V_y and V_z) using $V_x = V_r \cos\phi$ and $V_y = V_r \sin\phi$, where ϕ defines the angular position of each node of the Cartesian grid.

6) We constrain the minimum filament length by requiring that two age progressive volcanoes sample the same filament (Abouchami et al., 2005). A filament length of 300 km is insufficient and we favour a minimum length of 600 km.
7) We model the sudden arrival of Loa-type material (Tanaka et al., 2008) to investigate how Loa-side volcanoes change their geochemical signature over time. We show that such a long-lasting contribution (~3 Ma) implies the existence of isotopically distinct material with a vertical extent greater than 2000 km in the plume conduit.
8) Finally, we speculate on the relation between models of conduit structure and the sizes of heterogeneities in the thermal boundary layer (TBL) at the base of the Earth's mantle. Using the velocity field of Farnetani and Hofmann (2009), we advect the filaments backward in time until they are traced into the TBL. We find that a conduit structure with filaments implies the survival of heterogeneous material in the TBL with length-scales of several hundred kilometers in the radial and azimuthal directions. In contrast, a concentrically zoned conduit structure would map back into a horizontally stratified TBL, without radial and azimuthal geochemical variability (Farnetani and Hofmann, 2009).

Future numerical modelling will be needed to extend the insights gained here and to explore the dynamics of heterogeneities with distinct density and rheology. This will be particularly important for a fuller understanding of the behavior of eclogitic source components of mantle plumes. Future modelling may also address the mechanism(s) for generating the random, short-term fluctuations of magma composition, as well as the extreme compositional heterogeneities commonly seen in melt inclusions. We suggest that a much more detailed understanding of the physics of melt extraction will be needed to model these phenomena.

Acknowledgements

We thank Ross Kerr and an anonymous reviewer for constructive reviews, and Yanick Ricard for his editorial handling. C.G.F. thanks IDRIS (Orsay, France) for supercomputing facilities, and Claude Jaupart for support. We also appreciate many discussions with Alex Sobolev, Wafa Abouchami, Dominique Weis, and Bernhard Steinberger about Hawaii and with Francis Albarède and Janne Blichert-Toft on topics ranging from “stretched spaghetti” to “flying table cloths.” IPGP Contribution No. 2631; LDEO Contribution No. 7349.

References

Abouchami, W., Hofmann, A.W., Galer, S.J.G., Frey, F., Eisele, J., Feigenson, M., 2005. Pb isotopes reveal bilateral asymmetry and vertical continuity in the Hawaiian plume. Nature 434, 851–856.
Akima, H., 1996. Algorithm 760: rectangular-grid-data surface fitting that has the accuracy of a bicubic polynomial. ACM Trans. Math. Soft. 22, 357–361.
Bianco, T.A., Ito, G., van Hunen, J., Ballmer, M.D., Mahoney, J.J., 2008. Geochemical variation at the Hawaiian hot spot caused by upper mantle dynamics and melting of a heterogeneous plume. Geochem. Geophys. Geosyst. 9. doi:10.1029/2008GC002111.
Blichert-Toft, J., Frey, F.A., Albarède, F., 1999. Hf isotope evidence for pelagic sediments in the source of Hawaiian basalts. Science 285, 879–882.
Blichert-Toft, J., Weis, D., Maerschalk, C., Agranier, A., Albarède, F., 2003. Hawaiian hot spot dynamics as inferred from the Hf and Pb isotope evolution of Mauna Kea volcano. Geochem. Geophys. Geosyst. 4. doi:10.1029/2002GC000340.
Blichert-Toft, J., Albarède, F., 2009. Mixing and isotopic heterogeneities in the Mauna Kea plume conduit. Earth Planet. Sci. Lett. 282, 190–200.
Bourdon, B., Ribe, N.M., Stracke, A., Saal, A.E., Turner, S.P., 2006. Insights into the dynamics of mantle plumes from uranium-series geochemistry. Nature 444, 713–717.
Bryce, J.G., DePaolo, D.J., Lassiter, J.C., 2005. Geochemical structure of the Hawaiian plume: Sr, Nd, and Os isotopes in the 2.8 km HSDP-2 section of Mauna Kea volcano. Geochem. Geophys. Geosyst. 6. doi:10.1029/2004GC000809.
Connolly, J.A.D., Podladchikov, Y.Y., 2007. Decompaction weakening and channeling instability in ductile porous media: implications for asthenospheric melt segregation. J. Geophys. Res. 112. doi:10.1029/2005jb004213.
Coombs, M.L., Clague, D.A., Moore, G.F., Cousens, B.L., 2004. Growth and collapse of Waianae Volcano, Hawaii, as revealed by exploration of its submarine flanks. Geochem. Geophys. Geosyst. 5. doi:10.1029/2004GC000717.
Davies, G.F., 1988. Ocean bathymetry and mantle convection: 1. Large-scale flow and hotspots. J. Geophys. Res. 93, 10467–10480.
DePaolo, D.J., Stolper, E.M., 1996. Models of Hawaiian volcano growth and plume structure: implications of results from the Hawaii Scientific Drilling Project. J. Geophys. Res. 101, 11643–11654.
DePaolo, D.J., Bryce, J.G., Dodson, A., Shuster, D.L., Kennedy, B.M., 2001. Isotopic evolution of Mauna Loa and the chemical structure of the Hawaiian plume. Geochem. Geophys. Geosyst. 2. doi:10.1029/2000GC000139.
Detrick, R.S., Crough, S.T., 1978. Island subsidence, hot spots, and lithospheric thinning. J. Geophys. Res. 83, 1236–1244.
Eisele, J., Abouchami, W., Galer, S.J.G., Hofmann, A.W., 2003. The 320 ky Pb isotope evolution of the Mauna Kea lavas recorded in the HSDP-2 drill core. Geochem. Geophys. Geosyst. 4. doi:10.1029/2002GC000339.
Farnetani, C.G., Legras, B., Tackley, P.J., 2002. Mixing and deformations in mantle plumes. Earth Planet. Sci. Lett. 196, 1–15.
Farnetani, C.G., Hofmann, A.W., 2009. Dynamics and internal structure of a lower mantle plume conduit. Earth Planet. Sci. Lett. 282, 314–322.
Fekiacova, Z., Abouchami, W., Galer, S.J.G., Garcia, M.O., Hofmann, A.W., 2007. Origin and temporal evolution of Ko'olau volcano, Hawaii: inferences from isotope data on the Ko'olau Scientific Drilling Project (KSDP), the Honolulu volcanics and ODP Site 843. Earth Planet. Sci. Lett. 261, 65–83.
Garcia, M.O., Caplan-Auerbach, J., De Carlo, E.H., Kurz, M.D., Becker, N., 2006. Geology, geochemistry and earthquake history of Loìhi Seamount, Hawaii's youngest volcano. Chemie der Erde-Geochemistry 66, 81–108.
Hanano, D., Weis, D., Scoates, J.S., Aciego, S., DePaolo, D.J., 2010. Horizontal and vertical zoning of heterogeneities in the Hawaiian mantle plume from the geochemistry of consecutive postshield volcano pairs: Kohala–Mahukona and Mauna Kea–Hualalai. Geochem. Geophys. Geosyst. 11. doi:10.1029/2009GC002782.
Hauri, E.H., 1996. Major-element variability in the Hawaiian mantle plume. Nature 382, 415–419.
Hauri, E.H., Lassiter, J.C., DePaolo, D.J., 1996. Osmium isotope systematics of drilled lavas from Mauna Loa, Hawaii. J. Geophys. Res. 101, 11793–11806.
Herzberg, C., 2006. Petrology and thermal structure of the Hawaiian plume from Mauna Kea volcano. Nature 444, 605–609.
Holtzman, B.K., Kohlstedt, D.L., Zimmerman, M.E., Heidelbach, F., Hiraga, T., Hustoft, J., 2003. Melt segregation and strain partitioning: implications for seismic anisotropy and mantle flow. Science 301, 1227–1230.
Huang, S., Frey, F.A., 2003. Trace element abundances of Mauna Kea basalt from phase 2 of the Hawaii Scientific Drilling Project: petrogenetic implications of correlations with major element content and isotopic ratios. Geochem. Geophys. Geosyst. 4. doi:10.1029/2002GC000322.
Huang, S., Frey, F.A., Blichert-Toft, J., Fodor, R.V., Bauer, G.R., Xu, G., 2005. Enriched components in the Hawaiian plume: evidence from Kahoolawe Volcano, Hawaii. Geochem. Geophys. Geosyst. 6. doi:10.1029/2005GC001012.
Iwamori, H., McKenzie, D., Takahashi, E., 1995. Melt generation by isentropic mantle upwelling. Earth Planet. Sci. Lett. 134, 253–266.
Jackson, E.D., Silver, E.A., Dalrymple, G.B., 1972. Hawaiian–Emperor chain and its relation to Cenozoic circumpacific tectonics. Geol. Soc. Am. Bull. 83, 601–617.
Jin, Z.-M., Zhang, J., Green, H.W., Jin, S., 2001. Eclogite rheology: implications for subducted lithosphere. Geology 29, 667–670.
Karato, S.I., Wu, P., 1993. Rheology of the upper mantle: a synthesis. Science 260, 771–778.
Katz, R.F., Spiegelman, M., Langmuir, C.H., 2003. A new parametrization of hydrous mantle melting. Geochem. Geophys. Geosyst. 4. doi:10.1029/2002GC000433.
Kavner, A., 2007. Garnet yield strength at high pressure and implications for upper mantle and transition rheology. J. Geophys. Res. 112. doi:10.1029/2007JB004931.
Kerr, R.C., Mériaux, C., 2004. Structure and dynamics of sheared mantle plumes. Geochem. Geophys. Geosyst. 5. doi:10.1029/2004GC000749.
Kerr, R.C., Lister, J.R., 2008. Rise and deflection of mantle plume tails. Geochem. Geophys. Geosyst. 9. doi:10.1029/2008GC002124.
Laske, G., Morgan, J.-P., Orcutt, J.A., 2007. The Hawaiian SWELL pilot experiment. Evidence for lithosphere rejuvenation from ocean bottom surface wave data. In: Foulger, G.R., Jurdy, D.M. (Eds.), Plates, Plumes, and Planetary Processes: Geological Society of America Special Paper, 430, pp. 209–233.
Lassiter, J.C., DePaolo, D.J., Tatsumoto, M., 1996. Isotopic evolution of Mauna Kea volcano: results from the initial phase of the Hawaii Scientific Drilling Project. J. Geophys. Res. 101, 11769–11780.
Lassiter, J.C., Hauri, E.H., 1998. Osmium-isotope variations in Hawaiian lavas: evidence for recycled oceanic crust in the Hawaiian plume. Earth Planet. Sci. Lett. 164, 483–496.
Lipman, P.W., Sisson, T.W., Coombs, M.L., Calvert, A., Kimura, J.-I., 2006. Piggyback tectonics: long-term growth of Kilauea on the south flank of Mauna Loa. J. Volcanol. Geotherm. Res. 151, 73–108.
Manga, M., 1996. Mixing of heterogeneities in the mantle: effect of viscosity differences. Geophys. Res. Lett. 23, 403–406.
McKenzie, D., Bickle, M.J., 1988. The volume and composition of melt generated by extension of the lithosphere. J. Petrol. 25, 139–164.
Moore, J.G., Clague, D.A., 1992. Volcano growth and evolution of the island of Hawaii. Geol. Soc. Am. Bull. 104, 1471–1484.
Moore, W.B., Schubert, G., Tackley, P.J., 1998. Three-dimensional simulations of the plume–lithosphere interaction at the Hawaiian swell. Science 279, 1008–1011.
Morgan, W.J., 1971. Convection plumes in the lower mantle. Nature 230, 42–43.
Olson, P., Schubert, G., Anderson, C., 1993. Structure of axisymmetric mantle plumes. J. Geophys. Res. 98, 6829–6844.

Phipps Morgan, J., Morgan, W.J., Zhang, Y.-S., Smith, W.H.F., 1995. Observational hints for a plume-fed, suboceanic asthenosphere and its role in mantle convection. J. Geophys. Res. 100, 12753–12767.
Pietruszka, A.J., Garcia, M.O., 1999. Rapid fluctuation in the mantle source and melting history of Kilauea volcano inferred from the geochemistry of its historical summit lavas (1790–1982). J. Petrol. 40, 1321–1342.
Putirka, K.D., 2005. Mantle potential temperatures at Hawaii, Iceland, and the mid-ocean ridge system, as inferred from olivine phenocrysts: evidence for thermally driven mantle plumes. Geochem. Geophys. Geosyst. 6. doi:10.1029/2005GC000915.
Quane, S.L., Garcia, M.O., Guillou, H., Hulsebosch, T.P., 2000. Magmatic history of the east rift zone of Kilauea Volcano, Hawaii based on drill core from SOH 1. J. Volcanol. Geotherm. Res. 102, 319–338.
Ren, Z.-Y., Ingle, S., Takahashi, E., Hirano, N., Hirata, T., 2005. The chemical structure of the Hawaiian mantle plume. Nature 436, 837–840.
Ren, Z.-Y., Shibata, T., Yoshikawa, M., Johnson, K.T.M., Takahashi, E., 2006. Isotope compositions of submarine Hana Ridge lavas, Haleakala volcano, Hawaii: implications for source compositions, melting processes and the structure of the Hawaiian plume. J. Petrol. 47, 255–275.
Ribe, N.M., Christensen, U.R., 1994. Three-dimensional simulations of plume–lithosphere interaction. J. Geophys. Res. 99, 669–682.
Ribe, N.M., Christensen, U.R., 1999. The dynamical origin of Hawaiian volcanism. Earth Planet. Sci. Lett. 171, 517–531.
Richards, M.A., Griffiths, R.W., 1988. Deflection of plumes by mantle shear flow: experimental results and a simple theory. Geophys. J. 94, 367–376.
Robinson, J.E., Eakins, B.W., 2006. Calculated volumes of individual shield volcanoes at the young end of the Hawaiian Ridge. J. Volcanol. Geotherm. Res. 151, 309–317.
Sharp, W.D., Renne, P.R., 2005. The $^{40}Ar/^{39}Ar$ dating of core recovered by the Hawaii Scientific Drilling Project (phase 2), Hilo, Hawaii. Geochem. Geophys. Geosyst. 6. doi:10.1029/2004GC000846.
Sleep, N.H., 1990. Hotspot and mantle plumes: some phenomenology. J. Geophys. Res. 95, 6715–6736.
Sobolev, A.V., Hofmann, A.W., Nikogosian, I.K., 2000. Recycled oceanic crust observed in 'ghost plagioclase' within the source of Mauna Loa lavas. Nature 404, 986–989.
Sobolev, A.V., Hofmann, A.W., Sobolev, S.V., Nikogosian, I.K., 2005. An olivine-free mantle source of Hawaiian shield basalts the source of Mauna Loa lavas. Nature 434, 590–597.
Sobolev, A.V., Hofmann, A.W., et al., 2007. The amount of recycled crust in sources of mantle-derived melts. Science 316, 412–417.
Spiegelman, M., 1996. Geochemical consequences of melt transport in 2-D: the sensitivity of trace elements to mantle dynamics. Earth Planet. Sci. Lett. 139, 115–132.
Steinberger, B., O'Connell, R.J., 2003. Hotspot motion inferred from mantle flow models: implications on global plate reconstructions. Geophys. Res. Abstr. 5, 08130.
Steinberger, B., 2000. Plumes in a convecting mantle: models and observations for individual hotspots. J. Geophys. Res. 105, 11127–11152.
Steinberger, B., Sutherland, R., O'Connell, R.J., 2004. Prediction of Emperor–Hawaii seamount locations from a revised model of global plate motion and mantle flow. Nature 430, 167–173.
Tackley, P.J., 1998. Three-dimensional simulations of mantle convection with a thermo-chemical basal boundary layer: D″? The core–mantle boundary region. In: Gurnis, M. (Ed.), Geophys. Monogr. Ser., Vol. 28. AGU, pp. 231–253.
Tanaka, R., Makishima, A., Nakamura, E., 2008. Hawaiian double volcanic chain triggered by an episodic involvement of recycled material: constraints from temporal Sr–Nd–Hf–Pb isotopic trend of the Loa-type volcanoes. Earth Planet. Sci. Lett. 265, 450–465.
van Hunen, J., Zhong, S., 2003. New insights in the Hawaiian plume swell dynamics from scaling laws. Geophys. Res. Lett. 30. doi:10.1029/2003GL017646.
Watts, A.B., tenBrink, U.S., 1989. Crustal structure, flexure and subsidence history of the Hawaiian Islands. J. Geophys. Res. 94, 10473–10500.
Wirth, R., Rocholl, A., 2003. Nanocrystalline diamond from the Earth's mantle under Hawaii. Earth Planet. Sci. Lett. 211, 357–369.
Wolfe, C.J., Solomon, S.C., Laske, G., Collins, J.A., Detrick, R.S., Orcutt, J.A., Bercovici, D., Hauri, E.H., 2009. Mantle shear-wave velocity structure beneath the Hawaiian hot spot. Science 326, 1388–1390.